

Thermally Induced Elimination Reactions in Xerosols Derived from (Fluoroorgano)tin Compounds: A New Efficient Way To Prepare F-Doped Tin Dioxide Materials

Céline Franc, Bernard Jousseau, Manuela Linker, and Thierry Toupance*

Laboratoire de Chimie Organique et Organométallique, UMR 5802 CNRS, Université Bordeaux I, 351 Cours de la Libération, F33405 Talence Cedex, France

Received May 26, 2000. Revised Manuscript Received July 28, 2000

Trialkynyl(fluoroorgano)tins(IV) ($C_4H_9-C\equiv C)_3-SnR_F$ (**1**) ($R_F = -(CH_2)_2-CF_3$, $-o-FC_6H_4$) have been synthesized in three steps from tricyclohexyltin hydride or chloride and were characterized by multinuclear 1H , ^{13}C , ^{19}F , and ^{119}Sn NMR spectroscopy. Hydrolysis of **1** yielded oxo-hydroxyorganotin oligomers soluble in acetonitrile and alcohols, where each tin atom bears a fluorinated organic group. Thermally induced β - or γ -elimination reactions, evidenced by TG/MS measurements, allowed the insertion of fluorine into the oxide network and the removal of the undesirable organics. Densification at 550 °C gave crystalline particles of SnO_2 cassiterite containing the required amount of doping fluorine (4 at. %) and exhibiting an electronic resistivity ($0.3 \Omega \cdot cm$) lower than that previously reported ($2-10 \Omega \cdot cm$) for similar tin oxide materials. β - or γ -elimination processes in organotin compounds appear to be a suitable method of preparation of highly conductive nanocrystalline F-doped SnO_2 materials by the sol-gel route with low contaminating carbon content.

Introduction

Chemically or thermally induced β - and γ -elimination reactions are usually undesirable processes in organotin chemistry when the metal is linked to an organic group bearing heteroatoms such as oxygen or halogens.¹ Most studies have focused on the organic products released by the reactions. It is indeed an efficient method to prepare alkenes of controlled stereochemistry² and cyclopropanes.³ However, very few works have been devoted to highlight the organometallic counterpart. To our knowledge, it has only been used to generate organotin catalysts for silicone curing or polyurethane formation.⁴ On the other hand, doped tin dioxide materials find widespread applications in various fields. As thin films, they are present in modern electronic devices such as I.R. reflectors, electronic displays, and solar cells.⁵ Doped SnO_2 powders are used in preparation of transparent electrodes⁶ and as antistatic coatings

in paints or photographic films.⁷ It has been shown that fluorine is the most efficient doping agent leading to the highest electronic conductivity and I.R. reflectivity,^{5,8} but to our knowledge, no study has been conducted on the preparation of F-doped SnO_2 powders.

Among the different preparations described, the sol-gel process is well-suited to prepare oxide materials with very specific shapes and properties.⁹ This method consists of hydrolysis and condensation reactions of molecular precursors preforming an oxide network that is densified by thermal treatment. The route that involves the use of alkoxide precursors appears to be the more versatile one,¹⁰ but very few papers report on F-doped SnO_2 materials obtained by the sol-gel process.¹¹ We recently described alkoxyfluorodi(β -diketonate)tin complexes, including the Sn-F bond, which are sol-gel precursors of conductive F-doped SnO_2 powders.^{11b-c} However, the use of strong chelating β -diketonate ligands, necessary to obtain stable sols,¹²

* To whom correspondence should be addressed. E-mail: t.toupance@lcoo.u-bordeaux.fr.

(1) Davidson, P. J.; Lappert, M. F.; Pearce, R. *Chem. Rev.* **1976**, *76*, 219. (b) Kauffmann, T. *Angew. Chem., Int. Ed. Engl.* **1982**, *21*, 410. (c) Adcock, W.; Krstic, A. R.; Duggan, P. J.; Shiner, V. J., Jr.; Coope, J.; Ensiger, M. W. *J. Am. Chem. Soc.* **1990**, *112*, 3140. (d) Adcock, W.; Coope, J.; Shiner, V. J., Jr.; Trout, N. A. *J. Org. Chem.* **1990**, *55*, 1411. (e) Lambert, J. B.; Zhao, Y.; Emblidge, R. W.; Salvador, L. A.; Liu, X.; So, J.-H.; Chelius, E. C. *Acc. Chem. Res.* **1999**, *32*, 183.

(2) (a) Jousseau, B.; Noiret, N.; Pereyre, M.; Francès, J.-M. *J. Chem. Soc., Chem. Commun.* **1992**, 739. (b) Jousseau, B.; Noiret, N.; Pereyre, M.; Francès, J.-M.; Pétraud, M. *Organometallics* **1992**, *11*, 3910.

(3) Kuivila, H. G.; Scarpa, N. M. *J. Am. Chem. Soc.* **1970**, *92*, 6990.

(4) (a) Jousseau, B.; Gouron, V.; Maillard, B.; Pereyre, M.; Francès, J.-M. *Organometallics* **1990**, *9*, 1330. (b) Francès, J.-M.; Gouron, V.; Jousseau, B.; Pereyre, M. Eur. Patent 338947, 1989, 343086, 1989, 421895, 1991. (c) Jousseau, B.; Noiret, N.; Pereyre, M.; Saux, A. *Organometallics* **1994**, *13*, 1034.

(5) Chopra, K. L.; Major, S.; Pandya, D. K. *Thin Solid Films* **1983**, *102*, 1.

(6) (a) Goebbert, C.; Aegerter, M. A.; Burgard, D.; Nass, R.; Schmidt, H. *J. Mater. Chem.* **1999**, *9*, 253. (b) Cao, L.; Huo, L.; Ping, G.; Wang, D.; Zeng, G.; Xi, S. *Thin Solid Films* **1999**, *347*, 258.

(7) (a) Sonoda, N.; Shimotsu, W.; Tsubusaki, S. U.S. Patent, 4246143, 1981. (b) Robert, J. C. U.S. Patent, 5494652, 1996.

(8) Proscia, J.; Gordon, R. G. *Thin Solid Films* **1992**, *214*, 175.

(9) (a) Brinker, C. J.; Scherer, G. W. *Sol-Gel Science*; Academic Press: New York, 1990. (b) Chandler, C. D.; Roger, C. *Chem. Rev.* **1993**, *93*, 1205. (c) Corriu, R. J. P.; Leclercq, D. *Angew. Chem., Int. Ed. Engl.* **1996**, *35*, 1420.

(10) Livage, L.; Henry, M.; Sanchez, C. *Prog. Solid State Chem.* **1988**, *18*, 259.

(11) (a) Ray, S. C.; Karanjai, M. K.; DasGupta, D. *Surf. Coat. Technol.* **1998**, *102*, 73. (b) Gamard, A.; Jousseau, B.; Toupance, T.; Campet, G. *Inorg. Chem.* **1999**, *38*, 4671. (c) Gamard, A. Ph.D. Thesis, University Bordeaux I, 1999.

(12) Armelao, L.; Ribot, F. O.; Sanchez, C. *Better Ceramic Through Chemistry VII: Organic-Inorganic Hybrid Materials*; Coltrain, B., Sanchez, C., Schaefer, D. W., Wilkes, G. L., Eds.; Materials Research Society: Pittsburgh, PA, 1996; p 387.

induced the presence of contaminating carbon in the final materials.^{11c} An alternative to the route described above consists of the use of tin compounds with an organic group linked to the metal to provide good solubility of the hydrolyzed product and a source of tin-fluorine bond by thermal elimination. It should be a promising way both to introduce fluorine in tin oxide and to avoid polluting ligands.

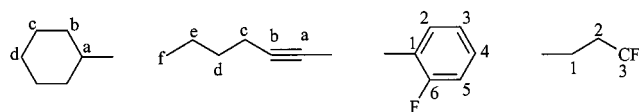
Thus, the aim of this work was to prepare organotin compounds with three hydrolyzable groups and a β - or γ -fluorinated organic group capable of giving a fluorine-tin bond by an elimination reaction. Alkynyl substituents were selected as hydrolyzable groups for the ease of purification of the corresponding organotin by column chromatography on Florisil¹³ instead of distillation at high temperature for liquid trialkoxytin derivatives, which could induce premature decomposition of the fluorinated chain. Tetraorganotins including β -substituted fluoroalkyl groups are known to be unstable at room temperature¹⁴ whereas the decomposition temperature is higher (150–200 °C) when the chain is perfluorinated.¹⁵ According to the literature, mono-¹⁶ or polyfluorophenyltriorganotins¹⁷ and 3,3,3-trifluoropropyltin compounds¹⁸ seems to be more stable than the previous derivatives. Consequently, we hereafter describe the synthesis and the hydrolytic and thermolytic behaviors of new molecular precursors ($C_4H_9-C\equiv C$)₃-SnR_F (**1**) (R_F = *o*-FC₆H₄, -(CH₂)₂CF₃) of F-doped SnO₂ materials.

Experimental Section

General Procedures, Starting Materials, and Instrumentation. Diethyl ether, *n*-pentane, THF, and toluene were distilled from sodium benzophenone ketyl prior to use. Dichloromethane and *n*-hexane were distilled over CaH₂. Propan-2-ol was distilled over CaSO₄. All solvents were stored over activated 4-Å molecular sieves under an atmosphere of nitrogen in a glass storage vessel fitted with a high-vacuum PTFE stopcock. 3,3,3-Trifluoroprop-1-ene (Aldrich) and 1-bromo-2-fluorobenzene (Fluorochem) were used as purchased. Tricyclohexyltin chloride¹⁹ and tricyclohexyltin hydride²⁰ were synthesized according to the literature methods.

Solution NMR analyses were performed on a Bruker AC-250 spectrometer or a Bruker DPX-200 spectrometer. ¹H NMR spectra were recorded at 250 MHz (solvent CDCl₃) while ¹³C NMR spectra were obtained at 62.9 MHz (solvent CDCl₃). Chemical shifts were referenced using the *protio* impurities (at 7.24 and 77 ppm in ¹H and ¹³C RMN, respectively) of the deuterated solvent. ¹¹⁹Sn NMR spectra were recorded at 74.6 MHz (solvent CDCl₃, reference Me₄Sn) and ¹⁹F NMR spectra at 188.3 MHz (solvent CDCl₃, reference CFCl₃). For NMR data, the multiplicity, coupling constants in Hz, and integration are given in parentheses. Tin-carbon coupling constants (Hz) are given in brackets. CP-MAS ¹¹⁹Sn NMR measurements were

carried out on a Bruker DPX 400 ($B_0 = 9.4$ T, $\omega/2 = 149.1514$ MHz) NMR spectrometer. A standard ZrO₂ rotor (4 mm) was used. The spectra were obtained by using conventional Hartmann-Hahn cross-polarization with contact times of 25 ms, acquisition times of 17 ms, and recycle delays of 10 s. Exponential multiplication of 100 Hz was applied before Fourier transformation. Infrared spectra (KBr pellets or disks) were recorded in the absorption mode using a FTIR Perkin-Elmer spectrophotometer. Mass spectrometry data were collected with a VG Autospec-Q working in the electronic impact mode. Elemental analyses were performed in the Center of Chemical Analysis of the CNRS (Vernaison, France). The water content was determined by the classical Karl-Fischer method with short time contact to avoid the titration of surface hydroxyl functions. Gel permeation chromatography (GPC) data were collected on a Waters system (510-type pump and 410-type refractometer, eluent THF at 1 mL min⁻¹, TSK GMHXL column porosity 1500–10⁷ Å). Average molecular weights were calculated using a third-order 12-points calibration curve obtained from polystyrene standards. The accuracy of the mass determination was checked with 3,3,3-trifluoropropyltricyclohexyltin.



3,3,3-Trifluoropropyltricyclohexyltin (3a). In a sealed tube, a mixture of tricyclohexyltin hydride (3.85 g, 10.4 mmol), 3,3,3-trifluoroprop-1-ene (4 g, 41.6 mmol), and AIBN (0.15 g, 0.9 mmol) was heated to 110 °C for 8 h. After cooling to room temperature, the white solids formed were dissolved in petroleum ether (200 mL) and the resulting solution was filtered. After solvent removal, the residue was recrystallized from absolute ethanol (100 mL) to give 4.09 g of white plates **3a** (yield: 85%); mp 163–165 °C.

¹H NMR (CDCl₃): δ 0.81 (part AA' of a AA'M₃XX' system, 2 H, H₁), 1.14–1.79 (m, 33 H, H_{a,b,c,d}), 2.10 (part XX' of a AA'M₃XX' system, 2 H, H₂). ¹³C{¹H} NMR (CDCl₃): δ -3 (q, ³J_{C-F} = 2, [229], C₁), 26.5 ([336], C_a), 27.5 (C_d), 29.6 ([54], C_c), 31.9 (q, ²J_{C-F} = 29, [11], C₂), 32.7 ([16], C_b), 127.7 (q, ¹J_{C-F} = 278, [66], C₃). MS-EI (*m/z*): 466 [M⁺]; 383 [M⁺ - C₆H₁₁]; 369 [M⁺ - C₃H₄F₃]; 301 [MH⁺ - 2C₆H₁₁]; 218 [MH⁺ - 3C₆H₁₁]; 203 [M⁺ - 2C₆H₁₁ - C₃H₄F₃]. Anal. Calcd for C₂₁H₃₇F₃Sn: C, 54.22; H, 8.02; F, 12.25; Sn, 25.51. Found: C, 53.53; H, 8.07; F, 12.08; Sn, 26.72.

2-Fluorophenyltricyclohexyltin (3b). In a three-necked flask under nitrogen, 15 mL (37.5 mmol) of 2.5 M butyllithium in hexane was slowly added to a solution of 1-bromo-2-fluorobenzene (7 g, 40 mmol) in dry diethyl ether (165 mL) at -80 °C. After this mixture was stirred at this temperature for 1 h, a solution of tricyclohexyltin chloride (19.3 g, 48 mmol) in 100 mL of THF was slowly added and the temperature was held at -80 °C for 3 h. After hydrolysis with a saturated solution of NH₄Cl, the mixture was extracted with petroleum ether (250 mL) and the organic phase was treated with a saturated solution of KF to remove unreacted tricyclohexyltin chloride. After filtration, the organic layer was washed with water (2 × 100 mL), dried over magnesium sulfate, and concentrated under vacuum. The obtained solids were recrystallized from absolute ethanol (850 mL) to give 12.05 g (26 mmol; yield: 85%) of white crystals **3b**. mp 184–185 °C.

¹H NMR (CDCl₃): δ 1.2–2.2 (m, 33 H, H_{a,b,c,d}), 7.1 (m, 1 H, H₃), 7.2 (m, 1 H, H₃), 7.4 (m, 1 H, H₄), 7.5 (m, 1 H, H₂). ¹³C{¹H} NMR (CDCl₃): δ 27.6 ([3], C_d), 27.9 ([354], C_a), 29.8 ([60], C_c), 32.7 ([16], C_b), 114.7 (d, ²J_{C-F} = 29, [15], C₅), 124.4 (d, ⁴J_{C-F} = 3, [30], C₃), 126.4 (d, ²J_{C-F} = 48, [266], C₁), 130.5 (d, ³J_{C-F} = 8, C₄), 138.3 (d, ³J_{C-F} = 16, [14], C₂), 167.6 (d, ¹J_{C-F} = 235, [10], C₆). MS-EI (*m/z*): 464 [M⁺]; 381 [M⁺ - C₆H₁₁]; 299 [MH⁺ - 2C₆H₁₁]; 215 [M⁺ - 3C₆H₁₁]; 196 [M⁺ - 3C₆H₁₁ - F]. Anal. Calcd for C₂₄H₃₇FSn: C, 62.22; H, 8.05; F, 4.10; Sn, 25.62. Found: C, 61.84; H, 7.90; F, 4.23; Sn, 24.65.

(13) Jaumier, P.; Jousseau, B.; Lahcini, M.; Ribot, F.; Sanchez, C. *J. Chem. Soc., Chem. Commun.* **1998**, 369.

(14) Akhtar, M.; Clark, H. C. *Can. J. Chem.* **1969**, *47*, 3753.

(15) Cullen, W. R.; Sams, J. R.; Waldam, M. C. *Inorg. Chem.* **1970**, *9*, 1682.

(16) (a) Tamborski, C.; Soloski, E. J.; Dee, S. M. *J. Organomet. Chem.* **1965**, *4*, 446. (b) Deacon, G. B.; Phillips, R. *J. Aust. J. Chem.* **1978**, *31*, 1709.

(17) (a) Deacon, G. B.; Gatehouse, B. M.; Nelson-Reed, K. T. *J. Organomet. Chem.* **1989**, *359*, 267. (b) Chen, J.-X.; Sakamoto, K.; Orita, A.; Otera, J. *J. Organomet. Chem.* **1999**, *574*, 58.

(18) (a) Murch, R. M. U.S. Patent, 3590060, 1971. (b) Williams, D. E.; Toporcer, L. H.; Ronk, G. M. *J. Phys. Chem.* **1970**, *74*, 2139.

(19) Pommier, J. C.; Pereyre, M.; Valade, J. C. *R. Acad. Sci.* **1965**, *260*, 6397.

(20) Jaumier, P. Ph.D. Thesis, University Bordeaux I, 1997.

3,3,3-Trifluoropropyltrichlorotin (2a). To a solution of **3a** (15.32 g, 32.9 mmol) in 45 mL of dry dichloromethane was added slowly tin tetrachloride (8.57 g, 32.9 mmol) under nitrogen. The reaction mixture was then refluxed overnight. After evaporation of the solvent, the residue was extracted for 4 h with a 1:1 mixture of acetonitrile:*n*-pentane (220 mL). The phases were separated under nitrogen and the acetonitrile solution was extracted with *n*-pentane (3 × 40 mL). All pentane phases were then washed with acetonitrile (3 × 40 mL) and the acetonitrile phases were gathered. Evaporation of the acetonitrile gave the trichloride, which was distilled in a Kugelrohr apparatus (bp 40 °C (0.2 mmHg)). A colorless oil (6.93 g, 19 mmol) was thus obtained (yield: 58%).

¹H NMR (CDCl₃): δ 2.34 (part AA' of a AA'M₃XX' system, 2 H, H₁), 2.69 (part XX' of a AA'M₃XX' system, 2H, H₂). ¹³C-{¹H} NMR (CDCl₃): δ 22.2 (q, ³J_{C-F} = 3, [771], C₁), 29.1 (q, ²J_{C-F} = 31, [46], C₂), 126 (q, ¹J_{C-F} = 277, C₃). MS-EI (*m/z*): 287 [M⁺ - Cl]; 267 [M⁺ - Cl - F]; 225 [M⁺ - C₃H₄F₃]; 155 [M⁺ - 2Cl - C₃H₄F₃].

2-Fluorophenyltrichlorotin (2b). The same procedure as that used for **2a** was followed with a solution of 16.96 g (37 mmol) of **3b** in 140 mL of *n*-pentane and 10.71 g (41 mmol) of tin tetrachloride. The desired product was purified by distillation in a Kugelrohr apparatus (bp 100 °C (0.05 mmHg)) to yield 7.43 g (23 mmol) of a colorless oil (yield: 63%).

¹H NMR (CDCl₃): δ 7.7 (m, 1 H), 7.8 (m, 1 H), 8.0–8.1 (m, 2 H). ¹³C-{¹H} NMR (CDCl₃): δ 116.4 (d, ²J_{C-F} = 23, [57], C₅), 121.9 (d, ²J_{C-F} = 34, C₁), 126.2 (d, ⁴J_{C-F} = 3, [53], C₃), 134.7 (d, ³J_{C-F} = 8, [37], C₂), 135.7 (d, ³J_{C-F} = 16, [15], C₄), 164.4 (d, ¹J_{C-F} = 244, [13], C₆). MS-EI (*m/z*): 320[M⁺]; 285 [M⁺ - Cl]; 250 [M⁺ - 3Cl]; 190 [M⁺ - Cl - C₆H₄F]; 155 [M⁺ - 2Cl - C₆H₄F].

(3,3,3-Trifluoropropyl)trihex-1-nyltin (1a). In a three-necked flask under nitrogen, 8 mL (20 mmol) of 2.5 M butyllithium in hexane was slowly added at 0 °C to a solution of 1.83 g (22.3 mmol) of hex-1-yne in THF/toluene: 1/1 (16 mL). After the reaction mixture was stirred at room temperature for 20 min, it was cooled to -80 °C and 2 g (6.2 mmol) of **2a** dissolved in THF/toluene: 1/1 (20 mL) was added dropwise. The mixture was allowed to return to room temperature and was then heated at 60 °C overnight. After filtration over dried MgSO₄ under nitrogen and evaporation of the solvent, the crude product was purified by column chromatography on Florisil (eluent: CH₂Cl₂). A yellow liquid was isolated (2 g, 4.8 mmol). Yield: 77%.

¹H NMR (CDCl₃): δ 0.90 (t, [7], 9 H, H₁), 1.2–1.5 (m, 14 H, H₁, and H_{e,d}), 2.25 (t, [7], 6 H, H_c), 2.35 (m, 2 H, H₂). ¹³C-{¹H} NMR (CDCl₃): δ 5.8 (q, ³J_{C-F} = 3, [636], C₁), 13.5 (C₇), 19.7 ([15], C₂), 21.9 (C₃), 29.9 (q, ²J_{C-F} = 31, [46], C₂), 30.5 (C₄), 75.9 ([893], C₆), 113 ([181], C₅), 127.3 (q, ¹J_{C-F} = 277, C₃). IR (KBr disks) ν (cm⁻¹) = 2963, 2937, 2875, 2162, 1595, 1467, 1440, 1430, 1320, 1264, 1206, 1173, 1113, 1064, 1025, 985, 952, 882, 830, 705. MS-EI (*m/z*): 379 [M⁺ - C₆H₉]; 363 [M⁺ - C₃H₄F₃].

2-Fluorophenyltrihex-1-nyltin (1b). In a three-necked flask under nitrogen, 8 mL (20 mmol) of 2.5 M butyllithium in hexane was slowly added at 0 °C to a solution of 1.83 g (22.3 mmol) of hex-1-yne in THF (20 mL). After the solution was stirred at room temperature for 20 min, the resulting solution was transferred via cannula to a funnel and was added dropwise at -80 °C to 2.38 g (7.4 mmol) of **2b** dissolved in THF/toluene: 1/1 (60 mL). The mixture was allowed to return to room temperature and was then heated at 60 °C overnight. The same purification procedure as that used for **1a** was followed. A yellow liquid was thus obtained (2 g, 4.6 mmol). Yield: 62%.

¹H NMR (CDCl₃): δ 0.88 (t, [7], 9H, H₁), 1.4–1.6 (m, 12 H, H_{e,d}), 2.27 (t, [7], 6H, H_c), 7.07 (m, 1 H), 7.19 (m, 1 H), 7.42 (m, 1 H), 7.60 (m, 1 H). ¹³C-{¹H} NMR (CDCl₃): δ 13.5 (C₇), 19.8 ([16], C₂), 21.8 (C₃), 30.4 ([9], C₄), 75.9 ([600], C₆), 112.7 ([200], C₅), 114.9 (d, ²J_{C-F} = 25, [21], C₅), 121.5 (d, ²J_{C-F} = 38, C₁), 124.6 (d, ⁴J_{C-F} = 3, [63], C₃), 132.3 (d, ³J_{C-F} = 8, C₂), 136.7 (d, ³J_{C-F} = 12, [31], C₄), 166.5 (d, ¹J_{C-F} = 240, C₆). IR (KBr disks) ν (cm⁻¹) = 2959, 2933, 2872, 2162, 1595, 1576, 1545, 1468, 1439, 1390, 1325, 1260, 1211, 1107, 1060, 1018, 970, 945,

855, 818, 762, 550, 537. MS-EI (*m/z*): 458[M⁺]; 377 [M⁺ - C₆H₉]; 363 [M⁺ - C₆H₄F]; 296 [M⁺ - 2C₆H₉]; 282 [M⁺ - C₆H₉ - C₆H₄F]; 215 [M⁺ - 3C₆H₉]; 201 [M⁺ - 2C₆H₉ - C₆H₄F].

Hydrolysis Experiments. To stirred **1** or Sn(C₆H₉)₄, a mixture of H₂O/propan-2-ol was slowly added to reach a hydrolysis ratio *h* equal to 8. After the mixture was stirred for 15 min at room temperature, the solvent and the volatile hydrolysis products were removed. The resulting powders were washed with dried *n*-hexane until the washing residue was colorless.

X₁, 1a: 1.82 g, 4 mmol. H₂O: 0.57 g, 32 mmol. Propan-2-ol: 5.77 g. After the solution was dried at 70 °C in vacuo, 1 g of a white powder was recovered.

Anal. Calcd for (C₃H₄F₃)(C₃H₇O)_{0.1}Sn(OH)_{0.2}O_{1.35}·0.9H₂O: C, 15.1; H, 2.6; F, 21.7; Sn, 45.1; H₂O, 6.2. Found: C, 15.2; H, 2.2; F, 21.6; Sn, 44.2; H₂O, 6.1.

X₂, 1b: 2.10 g, 4.6 mmol. H₂O: 0.66 g, 36.63 mmol. Propan-2-ol: 6.62 g. After the solution was dried at 70 °C in vacuo, 0.83 g of a white powder was recovered.

Anal. Calcd for (C₆H₄F)(C₃H₇O)_{0.1}Sn(OH)_{0.2}O_{1.35}·0.9H₂O: C, 29.0; H, 2.6; F, 7.3; Sn, 45.5; H₂O, 6.2. Found: C, 28.9; H, 2.5; F, 6.8; Sn, 45.0; H₂O, 6.0.

Thermolysis Experiments and Electrical Measurements. Thermal analyses were carried out on a Netzsch STA simultaneous analyzer. Thermogravimetry (TG) and derivative thermogravimetry (DTG) analyses were recorded in the range 50–650 °C under helium at a heating rate of 10 °C min⁻¹. Mass analyses were performed on a Thermostar Balzers Instruments quadrupole spectrometer. Powder samples were placed in alumina crucibles. Electron impact mass spectra (70 eV) were continuously recorded and stored, with scans from 3 to 300 amu. Each scan was recorded in 0.5 s with a delay time of 0.1 s. The coupled configuration (TG/MS) allowed us (i) to identify the evolved gaseous species from the total ion current as a function of *m/z* curves obtained from a recorded scan and (ii) to follow the ion current of a single proper *m/z* value that may represent the evolution, as a function of the temperature, of a particular molecular species.

The elimination reactions were also characterized as follows. In a Schlenk tube, 500 mg of xerosol X₁ was heated at 300 °C for 2 h under nitrogen. The gases released were trapped in a graduated flask filled with water. After cooling to room temperature, 10 mL of thermolysis products was recovered. The gas collected was then analyzed by gas chromatography (Hewlett-Packard 5890 chromatograph; column DBXLB; 30 m, *d* = 0.25 mm) coupled to mass spectrometry (VG autospec-Q; EI mode). Two main products were identified:

(1) 3,3,3-Trifluoroprop-1-ene (EI, *m/z*): 95 (M⁺ - H); 77 (M⁺ - F); 69 (CF₃⁺); 51 (CF₂H⁺); 27 (C₂H₃⁺).

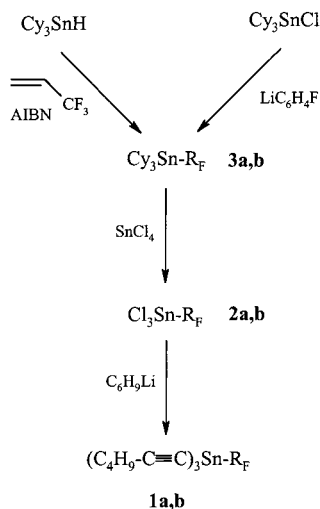
(2) 1,1-Difluorocyclopropane (EI, *m/z*): 77 (M⁺ - H); 59 (M⁺ - F); 51 (MH⁺ - C₂H₄); 27 (C₂H₃⁺).

Xerosols X₁ and X₂ were calcined in air at 550 °C for 15 min. Crystallinity of the powders was determined by powder X-ray diffraction using a Philips θ-2θ PW1820 diffractometer. The sample resistivity was estimated by compacting under pressure (10 ton) a given amount of powder (200 mg) between two stainless steel cylinders. The resistance *R_s* of the pelletized materials (13-mm diameter, 0.42-mm thickness) was measured with a Rhopoint M210 Milli-ohmmeter, under pressure (0.5 ton), using the previous cylinders as contacts. The sample resistivity ρ_s was deduced from *R_s* by the simple formula ρ_s = *SR_s*/*e* where *S* and *e* are the surface and the thickness of the sample, respectively.

Results and Discussion

Synthesis and Characterization of the Precursors. Compounds **1** were obtained by treatment of the corresponding trichloroorganotins **2** with 3 equiv of hex-1-nyllithium,^{13,21} as presented in Scheme 1. In the case of the aromatic compound, hex-1-nyllithium had to be

(21) Wrackmeyer, B.; Kehr, G.; Wettinger, D.; Milius, W. *Main Group Met. Chem.* **1993**, *16*, 445.

Scheme 1. Synthetic Pathway toward Trialkynyl(fluoroorgano)tin(IV) 1

a: $\text{R}_F = -(\text{CH}_2)_2\text{-CF}_3$

b: $\text{R}_F = -o\text{-FC}_6\text{H}_4$

slowly added to **2b**, the reverse procedure leading to decomposition products. Purification by column chromatography on Florisil gave analytically pure products in good yields (55–75%).

As far as compounds **2** are concerned, the synthesis of 3,3,3-trifluoropropyltin trichloride was already reported in the literature.^{18a} However, it was isolated from a redistribution reaction between tin tetrachloride and tetrakis(3,3,3-trifluoropropyl)tin with the concomitant formation of an equimolar amount of tris(3,3,3-trifluoropropyl)tin chloride as the byproduct. As this method leads to the waste of the fluorinated chains, monoorganotin **2** were more conveniently prepared²² from functional tricyclohexyltins **3** and tin tetrachloride. Purification by distillation under high vacuum produced the desired products in good yields (55–65%).

Derivatives **3** were obtained by hydrostannation of 3,3,3-trifluoroprop-1-ene by tricyclohexyltin hydride, either in the presence of a radical initiator or under UV irradiation, or by coupling of 2-fluorophenyllithium with tricyclohexyltin chloride. In the latter case, the substitution reaction must be conducted at -80°C to avoid elimination processes producing benzyne. The addition product of **3b** on benzyne was indeed isolated in experiments driven at -30°C or above. After recrystallization in absolute ethanol, tetraorganotin **3** were obtained in high yields (65–85%).

Compounds **1–3** were characterized by multinuclear NMR studies (Table 1). ^{119}Sn NMR chemical shift values are in good agreement with those expected.^{22,23} Resonances of trialkynyltin **1** are thus more shielded than those of tricyclohexylorganotin **3**, signals of trichlorides **2** showing the most pronounced downfield shift. Likewise, compounds bearing the *o*-fluorophenyl group exhibit more shielded resonances than the analogues including the 3,3,3-trifluoropropyl chain. In the ^{119}Sn NMR spectra, the key feature is the hyperfine structure

Table 1. ^{119}Sn and ^{19}F NMR Data of Compounds 1, 2, and 3

	δ ^{119}Sn (ppm) ^a	δ ^{19}F (ppm)	$J_{^{119}\text{Sn}-^{19}\text{F}}$ (Hz) ^b
3a	-67(s)	-70	unresolved
3b	-87(d)	-92	112
2a	-16(s)	-68	unresolved
2b	-63(d)	-93	138
1a	-244(q)	-69	7
1b	-291(d)	-93	127

^a s, singlet; d, doublet; q, quartet. ^b Determined from ^{119}Sn NMR spectra.

due to 3J (^{119}Sn – ^{19}F) couplings observed for most compounds studied. Only a few examples of ^{119}Sn – ^{19}F couplings through more than one bond were described.^{18b,24} In the 3,3,3-trifluoropropyl series, an unusual long-range coupling constant 4J was measured for **1a**, with a value slightly larger than those already reported for similar analogues.^{18b} Also, 3J (^{119}Sn – ^{19}F) coupling constants larger than 100 Hz were determined in the *o*-fluorophenyl series, with values 1 order of magnitude higher than those reported through saturated skeleton^{24a,b} and similar to 3J (^{119}Sn – ^1H) coupling measured in phenyltin derivatives.²³ The ^{19}F NMR chemical shifts of **1–3a** are equal to the one of trifluoropropane.²⁵ In contrast, those of **1–3b** are more than 10 ppm deshielded compared to the δ values tabulated for *o*-substituted benzene.²⁶

Intramolecular coordination of tin by a heteroatom, such as oxygen, located on a substituent of the metal atom, has been demonstrated in the case of trichlorostannyl ester and alcohols.^{22,27} However, the same phenomenon with fluorine is not well-documented. In the case of the 3,3,3-trifluoropropyl group, the NMR data are not consistent with a coordination of the tin atom by fluorine groups as already underlined by Williams et al.^{18b} This type of interaction cannot be completely excluded in the *o*-fluorophenyl series because a strong shift of the ^{19}F chemical shift was observed.

Hydrolytic Behavior and Characterization of the Xerosols. Compounds **1** were hydrolyzed in propan-2-ol according to the conditions settled in the case of functional trialkynyltins.¹³ After evaporation of the solvent and the volatile hydrolysis products, two xerosols X_1 and X_2 highly soluble in polar or coordinating solvents such as acetonitrile, tetrahydrofuran, and alcohols were obtained. Indeed, the lower functionality of **1** compared to tin molecules with hydroxyl groups or ligands^{11b,12} allowed condensed species exhibiting remarkable solubility properties to be prepared. To establish the nature of the condensed species formed, the IR, NMR, and TGA data of the as-prepared xerosols were collected.

In Figure 1 is shown the IR spectrum of X_1 , which indicates the tin–alkynyl bond cleavage and the concomitant formation of Sn–OH and Sn–O–Sn bonds. Indeed, the strong $\text{C}\equiv\text{C}$ stretching vibration at 2162

(24) (a) Clark, H. C.; Cyr, N.; Tsai, J. H. *Can. J. Chem.* **1967**, *45*, 1073. (b) Ulrich, S. E.; Zuckerman, J. J. *Inorg. Chim. Acta* **1979**, *34*, 161. (c) Adcock, W.; Kok, G. B.; Abeywickrema, A. N.; Kitching, W.; Drew, G. M.; Olszowsky, H. A.; Schott, I. *J. Am. Chem. Soc.* **1983**, *105*, 290. (d) Eujen, R.; Lagow, R. J. *J. Chem. Soc., Dalton Trans.* **1978**, 541.

(25) Weigert, F. J. *J. Org. Chem.* **1980**, *45*, 3476.

(26) Fifolt, M. J.; Sojka, S. A.; Wolfe, R. A.; Hojnicky, D. S.; Bieron, J. F.; Dinan, F. J. *J. Org. Chem.* **1989**, *54*, 3019.

(27) Biesemans, M.; Willem, R.; Damoun, S.; Geerlings, P.; Lahcini, M.; Jaumier, P.; Joussemaume, B. *Organometallics* **1996**, *15*, 2237.

(22) Joussemaume, B.; Lahcini, M.; Rasclé, M.-C.; Ribot, F.; Sanchez, C. *Organometallics* **1995**, *14*, 685.

(23) Wrackmeyer, B. *Annu. Rep. NMR Spectrosc.* **1985**, *16*, 73.

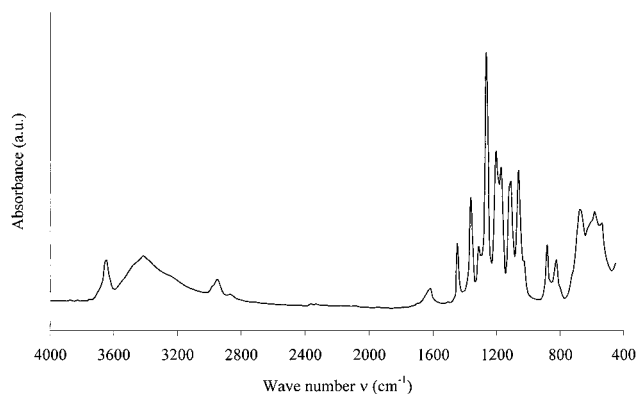


Figure 1. FTIR spectrum of xerosol X₁ after drying.

cm⁻¹ observed in the starting material **1a** disappeared completely and broad bands are found in the Sn–O stretching region (700 and 500 cm⁻¹).²⁸ Stretching modes at 3650 cm⁻¹ (sharp) and 3415 cm⁻¹ (very broad) are consistent with the presence of isolated and hydrogen-bonded surface hydroxyl groups, respectively, the corresponding deformation modes being centered at 1620 cm⁻¹.²⁹ Moreover, the peaks related to the C–H bond stretching centered at 2951 cm⁻¹, to the bending of the C–H bond in CH₂ at 1442 and 1361 cm⁻¹, and to the C–F bond stretching in CF₃ in the 1300–1150-cm⁻¹ region accounts for the presence of the 3,3,3-trifluoropropyl chain. The fluorinated group therefore seems to remain unaffected by the hydrolysis–condensation process. This was confirmed by the solution ¹⁹F NMR spectrum recorded in CD₃CN, which exhibits broadened resonances around –69 ppm in the same chemical shift range as that for **1a**, and by elemental analysis, which yields the following atomic ratios F/Sn = 3.05 and C/Sn = 3.4. As shown in the next section, the slight excess of carbon found is likely due to the small amount of propan-2-oxy groups remaining in X₁. Consequently, according to the microanalysis, the following formula (C₃H₄F₃)(C₃H₇O)_{0.1}Sn(OH)_{0.2}O_{1.35}·0.9H₂O may be proposed for xerosol X₁. This formula is in rather good agreement with the TG results. Indeed, TG–DTG of the xerosol carried out in air showed a mass loss occurring in three successive steps of 5.1, 34.2, and 2.1%, centered at 110, 295, and 420 °C, respectively, to give a final residue of 58.6% (expected: 57.3%).

As far as X₂ is concerned, the atomic ratios F/Sn = 0.95 and C/Sn = 6.3 were found by elemental analysis and a broad resonance around –93 ppm, close to the one of the precursor **1b**, was obtained by ¹⁹F NMR spectroscopy. As for X₁, bands characteristic of Sn–OH and Sn–O–Sn stretching vibrations were detected by IR spectroscopy but, also, these of the *o*-fluorophenyl group at 3065 cm⁻¹ (ν(C–H)), at 1594, 1577, 1469, and 1437 cm⁻¹ (ν(C=C)), at 1208 cm⁻¹ (ν(C–F)), at 1107 and 1054 cm⁻¹ (δ_{In-plane}(C–H)), and at 756 cm⁻¹ (δ_{Out-of-plane}(C–H)). Consequently, taking into account that the small excess of carbon is probably due to propan-2-oxy groups, the following formula (C₆H₄F)(C₃H₇O)_{0.1}Sn(OH)_{0.2}O_{1.35}·0.9H₂O can be proposed for X₂. The TG–DTG of X₂ carried out in air exhibited a continuous mass

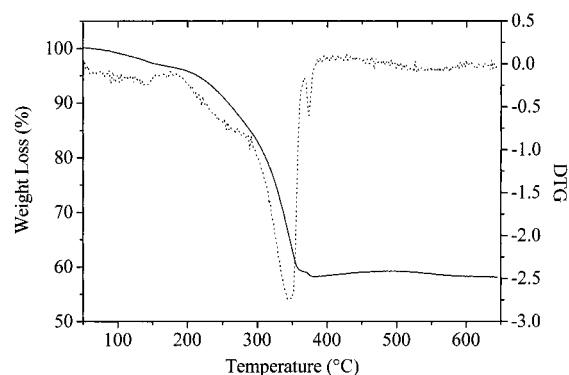


Figure 2. TGA plot of xerosol X₁ between 50 and 650 °C recorded at 5 °C min⁻¹.

loss of 39.8% centered at 242 °C, to give a final residue of 60.2%, close to the one expected (57.9%).

To determine the coordination of the tin atom, solution ¹¹⁹Sn NMR analyses were tentatively made, but the species formed gave no resonance. The latter could be ill-defined oligomeric or polymeric entities, which are not observed by solution ¹¹⁹Sn NMR because of their long reorientation times.³⁰ CP-MAS ¹¹⁹Sn NMR measurements were therefore performed on X₁. The spectrum, which is poorly resolved, exhibits two isotropic chemical shifts associated with their pattern of spinning sidebands. The major one is located around –370 ppm and the minor at –430 ppm, values falling into the region of five- or six-coordinate monoalkyltin atoms. Thus, the oxo-hydroxobutyltin cluster {(BuSn)₁₂O₁₄-(OH)₆}(OH)₂ is characterized in solid-state ¹¹⁹Sn NMR by two resonances at –280 and –450 ppm, which were ascribed to five- and six-coordinate tins, respectively.³¹

On the basis of GPC investigations, the average molecular weight of the species obtained was estimated to be 900 and 700 (±10% error) for xerosols X₁ and X₂, respectively. These values would indicate that these species would contain around three or four tin atoms. In summary, within experimental uncertainties, all the results are consistent with the formation of oxo-hydroxoorganotin entities, each tin atom being linked to a 3,3,3-trifluoropropyl or a *o*-fluorophenyl group.

Xerosol Pyrolysis. To study the conversion of the xerosols into densified powders, the pyrolysis of X₁ and X₂ was followed under helium flow by thermogravimetry coupled to mass spectrometry, an efficient technique to draw the reactions involved during the pyrolysis and the nature of the organics in sol–gel materials.³²

Under these conditions, the TG analysis of X₁ shows a continuous mass loss from 50 to 650 °C (Figure 2). Four mass losses, the second being the most conspicuous, were observed on TG traces and the main molecules detected by MS measurements were water (*m/z* = 18), hydrofluoric acid (*m/z* = 20), carbon dioxide (*m/z* = 44), propan-2-ol (*m/z* = 60), 1,1-difluorocyclopropane (*m/z* = 77), and 3,3,3-trifluoroprop-1-ene (*m/z* = 96) (Table 2).

(28) Giuntini, J. C.; Granier, W.; Zanchetta, J. V.; Taha, A. *J. Mater. Sci. Lett.* **1990**, *9*, 1383.

(29) Harrison, P. G.; Guest, A. *J. Chem. Soc., Faraday Trans. 1* **1987**, *83*, 3383.

(30) (a) Banse, F. Ph.D. Thesis, University Paris VI, 1994. (b) Eychenne-Baron, C.; Ribot, F.; Sanchez, C. *J. Organomet. Chem.* **1998**, *567*, 137.

(31) (a) Banse, F.; Ribot, F.; Tolédano, P.; Maquet, J.; Sanchez, C. *Inorg. Chem.* **1995**, *34*, 6371. (b) Ribot, F.; Banse, F.; Diter, F.; Sanchez, C. *New J. Chem.* **1995**, *19*, 1145.

(32) (a) Belot, V.; Corriu, R. J. P.; Leclercq, D.; Mutin, P. H.; Vioux, A. *J. Mater. Sci. Lett.* **1990**, *9*, 1052. (b) Di Maggio, R.; Campostrini, R.; Guella, G. *Chem. Mater.* **1998**, *10*, 3839.

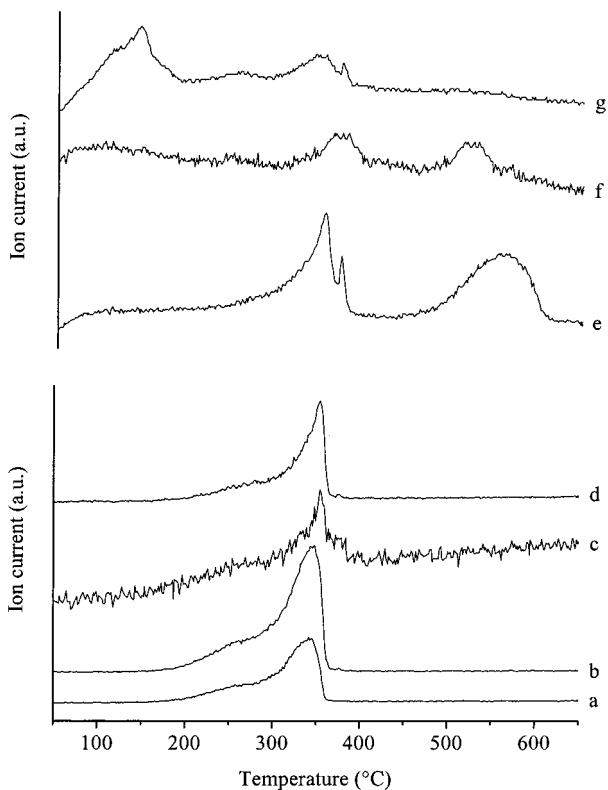


Figure 3. Xerosol X₁ *m/z* curves as a function of temperature. (a) 96 (CF₃CHCH₂); (b) 77 (CF₂CH₂CH₂); (c) 60 (CH₃CHOHCH₃); (d) 59; (e) 44 (CO₂); (f) 20 (HF); (g) 18 (H₂O).

Table 2. TGA Coupled with MS Data for Xerosol X₁

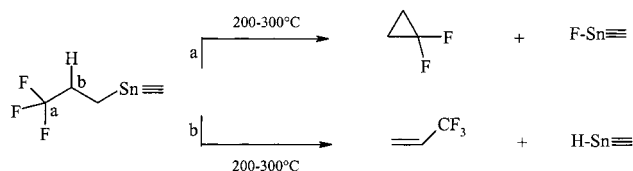
pyrolysis step	sampling temperature (°C)	mass loss intensity (%)	species detected
I	140	4	H ₂ O
II	345	36.1	H ₂ O, HF, CO ₂ , C ₃ H ₇ OH, C ₃ H ₄ F ₂ , C ₃ H ₃ F ₃
III	375	0.7	HF, CO ₂ , CF ₃ OH
IV	530	1.8	HF, CO ₂

In addition, no significant amount of ion fragment *m/z* = 81 was detected, confirming that most of the alkyne groups were removed upon hydrolysis.

The first weight loss at 140 °C is mainly assignable to the release of H₂O, probably trapped into the porosity of the xerosol, despite the drying step at 70 °C under vacuum (Figure 3g). The second contribution to the release of water occurs at 345 °C and probably comes from the condensation of Sn–OH moieties with the formation of oxo bridges, as was proposed in the case of gels prepared from modified zirconium *n*-butoxide.^{32b}

The large mass loss at 345 °C mainly corresponds to the elimination of the fluorinated chain as evidenced by the 96 *m/z*, 77 *m/z*, and 59 *m/z* ions versus temperature profiles (Figure 3a, b, and d). The two first ion fragments are characteristic of 3,3,3-trifluoroprop-1-ene and the two last are consistent with the formation of 1,1-difluorocyclopropane. The formation of the former product can be rationalized by postulating a β-elimination of hydrogen, leading to the creation of Sn–H bonds, which could rapidly decompose into Sn–O bonds in the presence of water at such temperature. On the other hand, γ-elimination of fluorine induces the formation of Sn–F bonds and 1,1-difluorocyclopropane (Scheme 2). With the aim to assess this interpretation, xerosol X₁

Scheme 2. Thermolysis Products of Xerosol X₁ Treated at 300 °C



was thermolyzed for 2 h at 300 °C and the nature of the released gases was checked by gas chromatography coupled to mass spectrometry. As expected, two main products were detected, 3,3,3-trifluoroprop-1-ene and 1,1-difluorocyclopropane in about a 2/3 molar ratio. At this stage, it can be concluded that γ-elimination of fluorine does take place and starts from 200 °C according to Figure 3b. It must also be underlined that although this elimination was not the only reaction, it took place at a sufficient rate for introducing a suitable amount of fluorine imparting low resistivity to tin dioxide materials. In addition, propan-2-ol was released from 200 to 350 °C as shown by the 60 *m/z* ion versus temperature profile (Figure 3c). This rather high-temperature process is in favor of the presence of propan-2-oxy groups in the xerosol, which validates the chemical formula proposed for X₁ (see above). The origin of such tin substituents can be rationalized by postulating an alcoholysis reaction occurring between propan-2-ol and Sn–alkynyl bonds during the hydrolysis step.¹³

The minor, but well-defined, mass loss at 375 °C can be ascribed to the departure of carbon dioxide and hydrofluoric acid. Finally, residual carbon (as CO₂) and fluorine (as HF) releases are responsible for the last mass loss around 530 °C (Figure 3e,f).

According to Figure 3e, fluorine loss occurs as hydrofluoric acid in two steps, around 350 and 530 °C, respectively. The former is associated with the decomposition of the fluoroorganic chain whereas the latter is probably due to the hydrolysis of the Sn–F bonds, generated by the γ-elimination reaction, in the presence of traces of water as was recently pointed out for xerosols prepared from alkoxyfluorodi(β-diketonate)tin complexes.³³ In this respect, it is worthwhile to note that this process is catalytic because it gives rise to Sn–OH groups, which react via an oxolation reaction to form water again. Detection of fluorine after the complete removal of the organic chain is therefore in favor of the creation of Sn–F bonds via a γ-elimination reaction.

The thermolytic behavior of X₂ is noticeably different from the previous one. The TG analysis of X₂ indeed indicates a continuous loss from 50 to 650 °C, with a maximum at 290 °C, without different stages being clearly distinguished. MS measurements revealed the removal of water, carbon dioxide, propan-2-ol, benzyne (*m/z* = 76), and *o*-fluorobenzene (*m/z* = 96) but, surprisingly, neither fluorine nor hydrofluoric acid was detected. In Figure 4 is shown the 96, 76, and 60 ion fragment versus temperature profiles, allowing the TG/DTG data to be highlighted.

As for X₁, propan-2-oxy groups are likely present in X₂. The striking feature is the loss of the fluorinated aromatic unit as fluorobenzene and benzyne, a process

(33) Gamard, A.; Babot, O.; Jousseau, B.; Rasclé, M.-C.; Toupance, T.; Campet, G. *Chem. Mater.*, in press.

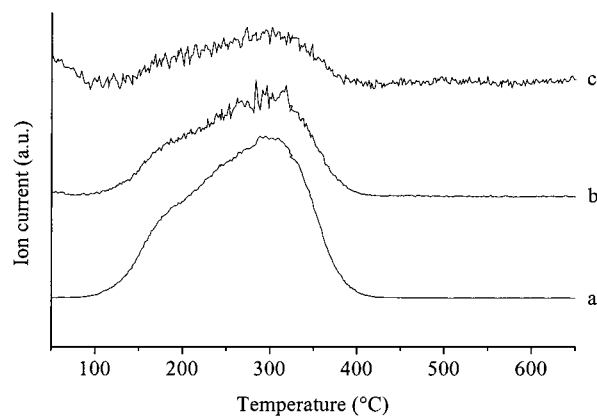


Figure 4. Selected m/z curves as a function of temperature for xerosol X_2 . (a) 96 (C_6H_5F); (b) 76 (C_6H_4); (c) 60 ($CH_3-CHOHCH_3$).

starting from a relatively low temperature, i.e., 100 °C. Consequently, partial decomposition of the aromatic unit during the drying step could account for the slight lack of fluorine in X_2 pointed out by elemental analysis. In comparison with the behavior of X_2 , these findings may be interpreted, on one hand, by the lower stability of the Sn–C_{ar} bond susceptible to cleavage by the Sn–OH group and, on the other hand, by β -elimination reactions, which are known to occur at lower temperatures than γ -elimination. Thus, benzyne would come from β -fluoride elimination, even if, in contrast to X_2 , TG/MS measurements did not provide clues about the creation of Sn–F bonds. It must also be remarked that pyrolysis of the organics takes place over a wide temperature range, i.e., from 100 to 350 °C, which is consistent with the rather slow reaction at low temperature.

Characterization of the Calcined Xerosols. Crystallization of tin dioxide particles is a prerequisite to obtain highly conductive F-doped materials.^{7,11b} In the case of powders prepared by the sol–gel route, thermal treatment below 400 °C gave poorly crystallized materials.^{11b} With xerosols X_1 and X_2 , annealing at 550 °C for 15 min led to the formation of crystalline materials. X-ray patterns of the resulting powders are characteristic of nanocrystalline particles of SnO₂ cassiterite (Figure 5).³⁴ The crystalline domains were estimated to be 7 nm by using the conventional Laue–Scherrer formula.³⁵ Transmission electron micrographs (TEM) show agglomerated nanoparticles with sizes in general agreement with the XRD determinations. It must also be noted that there was considerable distribution in size and that many particles exhibited irregular shapes.

Resistance measurements were then performed to estimate the conductivity of the materials (Table 3). Thermally treated xerosols X_1 and X_2 exhibited resistivity several orders of magnitude lower than that measured for commercial SnO₂ (Aldrich) powders, which can be explained by the migration of fluorine toward tin atoms in the materials through β - or γ -elimination

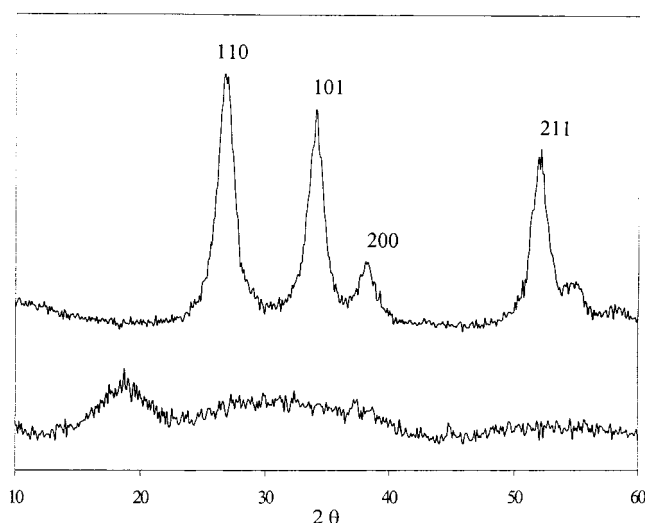


Figure 5. X-ray diffraction patterns of xerosol X_1 after thermal treatment at bottom (50 °C) and top (550 °C).

Table 3. Resistivity ρ , Crystallite Size (t), and Composition of the Different SnO₂ and F:SnO₂ Materials Studied (All Materials Were Treated at 550 °C and the Atomic Ratios F/Sn and C/Sn Were Determined by Elemental Analysis)

precursor	xerosol	ρ ($\Omega\cdot\text{cm}$)	t (nm) ^a	F/Sn	C/Sn	ref
1a	X_1	0.3	7	0.05	<0.03	<i>b</i>
1b	X_2	10	7	0.04	<0.03	<i>b</i>
SnF(OR)(acac) ₂	<i>c</i>	0.8	8	0.06	0.12	11c, 33
SnO ₂ (Aldrich)		2×10^3	50			<i>b</i>

^a Determined according to ref 35. ^b This study. ^c The xerosol was obtained according to a procedure described in ref 11c.

reaction. Atomic F/Sn ratios of 0.05–0.04 found by elemental analysis were in the range of the best doping amount, leading to the highest conductivity.³⁶ Another striking feature of these results was the low carbon amount of these powders, less than 4 times lower than that in materials prepared from alkoxyfluorodi(β -diketonate)tin complexes.^{11c} In this respect, these results corroborate the approach chosen, which involves a well-defined elimination reaction favoring the clean removal of the organics during the pyrolysis.

Xerosol X_1 treated at 550 °C gave rise to the lowest resistivity ever reported for F-doped SnO₂ powders.^{11b–c} Besides, the resistivity of this highly conductive nanocrystalline F-doped SnO₂ powder was 1 order of magnitude lower than that described for Sb-doped SnO₂ powders.⁷ The higher resistivity measured in the case of xerosol X_2 was quite unexpected because the chemical composition was close to the one described for xerosol X_1 . It could be due to the differences between X_1 and X_2 found for the fluorine loss by TG/MS analyses.

Conclusions

New trialkynyl(fluoroorgano)tin(IV) ($C_4H_9-C\equiv C$)₃–SnR_F (R_F = $C_3H_4F_3$, *o*-FC₆H₄) **1** compounds have been synthesized and characterized by multinuclear NMR spectroscopy. Hydrolysis–condensation processes removed the alkynide groups without affecting the Sn–R_F bond and provided soluble oxo-hydroxo stannic

(34) Powder diffraction file; J.C.P.D.S. International Center for Diffraction Data: Swarthmore, PA, 1997; no. 41-1445.

(35) The mean particle size is deduced from the bandwidth of the different peaks. See ref 11b and also Eberhardt, J. P. *Structural and Chemical Analysis of Materials*; John-Wiley & Sons: New York, 1991; p 203.

(36) The best doping amount is comprised between 1 and 8 at. % F per Sn atom. See ref 8 and also Fantini, M.; Torriani, I. *Thin Solid Films* **1986**, *138*, 255.

oligomers endowed with fluorinated organic groups after solvent removal.

TG/MS measurements afforded some insights into the reactions occurring during the pyrolysis step of these oxide species: (1) the trifluoropropyl chain is released from 200 to 350 °C as 3,3,3-trifluoroprop-1-ene and 1,1-difluorocyclopropane; (2) the *o*-fluorophenyl unit thermolyzes from a lower temperature, 100 °C, as *o*-fluorobenzene and benzyne; (3) in the case of the 3,3,3-trifluoropropyl unit, hydrofluoric acid is emitted in two stages around 350 and 530 °C, respectively. These results demonstrate that thermolysis of the xerosols resulted in β - or γ -elimination reactions, leading to the insertion of fluorine in the tin dioxide network.

The sample thermally densified in air at 550 °C gave nanocrystalline particles of SnO₂ cassiterite including the required amount of doping fluorine and exhibiting electronic resistivity lower (0.3 $\Omega\cdot\text{cm}$) than that previ-

ously reported for similar tin oxide materials (2–10 $\Omega\cdot\text{cm}$). The approach developed in this paper, which exploits well-defined thermally induced elimination reactions, appears to be a suitable preparation method of highly conductive nanocrystalline F-doped SnO₂ materials by the sol-gel route with a low content of contaminating carbon. The solubility of the xerosol obtained after hydrolysis should allow one to prepare F-doped SnO₂ thin films by dip- or spin-coating techniques.

Acknowledgment. Dr. G. Campet and Dr. M. Birot are acknowledged for helpful discussions, XRD measurements, and GPC analyses. The authors are indebted to Dr. I. Pianet for the CP-MAS ¹¹⁹Sn NMR measurements. Mrs. Babot, Sellier, and Vitry and Mr. Barbe and Petraud are thanked for their precious assistance.

CM001097R